Design, Preparation, and Electronic Structure of High-Spin Cation Diradicals Derived from Amine-Based Spin-Polarized Donors

Hiromi Sakurai,[†] Akira Izuoka,[‡] and Tadashi Sugawara*

Contribution from the Department of Basic Science, Graduate School of Arts and Sciences, The University of Tokyo, 3-8-1 Komaba, Meguro, Tokyo 153-8902, Japan

Received December 30, 1999

Abstract: Amine-based donor radicals, such as dimethylamino-, diethylamino- and morpholinonitronyl nitroxides, were synthesized, and their donor abilities were examined by cyclic voltammetry. ESR spectra of the singly oxidized donor radicals showed ground state triplet signals derived from the cation radicals of these donor radicals. The result was interpreted by the presence of the ferromagnetic coupling between the generated π-spin and the localized unpaired electron on the radical unit. According to the molecular orbital calculations, the ferromagnetic coupling between these two spins is originated from the space-sharing nature between SOMO which is localized on the radical unit and SOMO′ which is derived from HOMO of the donor radical upon one-electron oxidation. Therefore, the cation-radicals of these donor radicals can be regarded as a heteroanalogue of trimethylenemethane. *p*- and *m*-dimethylaminophenyl nitronyl nitroxides were synthesized in order to expand the π-electronic structure of the donor unit, and the singly oxidized species were also found to afford triplet ESR signals. The origin of the ferromagnetic coupling of these aminophenyl nitronyl nitroxides was discussed on the same basis. Charge transfer complexes of some of the donor radicals with chloranil or 2,3-dichloro-5,6-dicyano-1,4-benzoquinone were prepared, and the conducting and magnetic properties were examined.

Introduction

Molecular magnetism has originated from the discovery of the ground state quartet *m*-dicarbene, *m*-phenylenebis(phenylmethylene),[1] and has been developed rapidly during these two decades.[2] The high-spin state of *m*-dicarbene is derived from two types of strong ferromagnetic couplings: one is a one-centered exchange interaction at the divalent carbon atoms, and the other is a multicentered exchange interaction in the *m*-phenylene unit having two degenerated nonbonding molecular orbitals (NBMOs). The latter interaction aligns a pair of triplet spins at the carbenic carbon atoms ferromagnetically, giving rise to a ground state quintet species. Until now, a number of high-spin polycarbenes and polyradicals with a *m*-phenylene skeleton have been reported as the fruitful result of skillful synthetic efforts.[3] While a *m*-phenylene unit is frequently used as a ferromagnetic coupler in the preparation of high-spin molecules, there is a more basic diradical, that is, trimethylenemethane (**TMM**), of which the ground state is determined to be triplet, both experimentally[4] and theoretically.[5] For innovating a spin system which can be modulated by external stimuli, we have chosen **TMM** as the fundamental skeleton and intend to modify the basic **TMM** spin system in accord with the advanced purpose.

Since the intrinsic character of an organic spin system is that unpaired electrons occupy π-orbitals, modulation of the π-system is expected to control the magnetic interaction between unpaired electrons in π-orbitals.[6] The reason we are interested in a heteroanalogue of **TMM** for the above purpose is 2-fold. First, by introducing an oxidizable core (e.g., a dimethylamino group) into one of the peripheral carbon atoms, one can generate a diradical species by one-electron oxidation (Scheme 1, Step 1). Second, the remaining allyl radical unit can be stabilized substantially by replacing a heteroatom-centered radical source (e.g., nitronyl nitroxide) (Scheme 1, Step 2). The resultant heteroanalogue of **TMM** is **DMANN**$^{+\bullet}$ which can to be generated by one-electron oxidation of a nitronyl nitroxide derivative with a dimethylamino group (**DMANN**).

In this paper, we describe the molecular design and prepara-

[†] Present address: Japan Association for International Chemical Information (JACI).

[‡] Present address: Department of Chemistry, Faculty of Science, Ibaraki University.

(1) (a) Itoh, K. *Chem. Phys. Lett*. **1967**, *1*, 235−238. (b) Wasserman, E.; Murray, R. W.; Yager, W. A.; Trozzolo, A. M.; Smolinsky, G. *J. Am. Chem. Soc*. **1967**, *89*, 5076−5078.

(2) (a) *Magnetic Properties of Organic Materials*; Lahti, P. M., Ed.; Marcel Dekker: New York, 1999. (b) Rajca, A. *Chem. Rev*. **1994**, *94*, 871−893. (c) Miller, J. S.; Epstein, A. J. *Angew. Chem., Int. Ed. Engl*. **1994**, *33*, 385−415. (d) Gatteschi, D. *Adv. Mater*. **1994**, *6*, 635−645. (e) Kollmar, C.; Kahn, O. *Acc. Chem. Res*. **1993**, *26*, 259−265. (f) Dougherty, D. A. *Acc. Chem. Res*. **1991**, *24*, 88−94. (g) Iwamura, H. *Adv. Phys. Org. Chem*. **1990**, *26*, 179−253.

(3) (a) Rajca, A.; Rajca, S.; Wongsriratanakul, J. *J. Am. Chem. Soc*. **1999**, *121*, 6308−6309. (b) Matsuda, K.; Nakamura, N.; Inoue, K.; Koga, N.; Iwamura, H. *Bull. Chem. Soc. Jpn*. **1996**, *69*, 1483−1494. (c) Wienk, M. M.; Janssen, R. A. J. *J. Am. Chem. Soc*. **1997**, *119*, 4492−4501. (d) Selby, T. D.; Blackstock, S. C. *J. Am. Chem. Soc*. **1998**, *120*, 12155−12156. (e) Nishide, H.; Miyasaka, M.; Tsuchida, E. *Angew. Chem., Int. Ed*. **1998**, *37*, 2400−2402. (f) Bushby, R. J.; Gooding, D. *J. Chem. Soc., Perkin Trans. 2* **1998**, 1069−1075. (g) Lahti, P. M.; Esat, B.; Walton, R. *J. Am. Chem. Soc*. **1998**, *120*, 5122−5123. (h) Sato, K.; Yano, M.; Furuichi, M.; Shiomi, D.; Takui, T.; Abe, K.; Itoh, K.; Higuchi, A.; Katsuma, K.; Shirota, Y. *J. Am. Chem. Soc*. **1997**, *119*, 6607−6613.

(4) (a) Baseman, R. J.; Pratt, D. W.; Chow, M.; Dowd, P. *J. Am. Chem. Soc*. **1976**, *98*, 5726−2727. (b) Wenthold, P. G.; Hu, J.; Squires, R. R.; Lineberger, W. C. *J. Am. Chem. Soc*. **1996**, *118*, 475−476.

(5) Feller, D.; Borden, W. T.; Davidson, E. R. *J. Chem. Phys.* **1981**, *74*(4), 2256−2259.

(6) (a) Ishiguro, K.; Ozaki, M.; Sekine, N.; Sawaki, Y. *J. Am. Chem. Soc*. **1997**, *119*, 3625−3626. (b) Matsuda, K.; Irie, M. *Chem. Lett*. **2000**, 16−17. (c) Hamachi, K.; Matsuda, K.; Iwamura, H. *Bull. Chem. Soc. Jpn*. **1998**, *71*, 2937−2943.

10.1021/ja994547t CCC: $19.00
Published on Web 09/21/2000

Scheme 1. Molecular Design for a Heteroanalogue of TMM

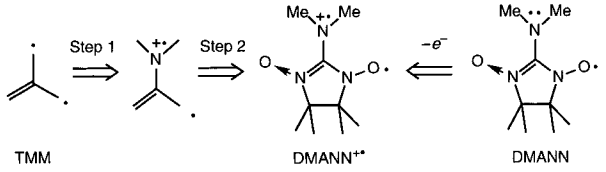

Scheme 2. Preparation of (a) Amine-Based Donor Radicals and (b) Aminophenyl-Based Donor Radicals

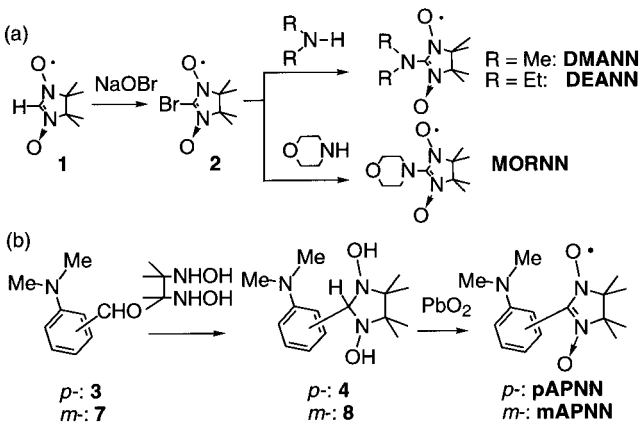

tion of amine-based donor radicals in which a radical unit is connected with a donor unit in a cross-conjugating manner. It turned out that one-electron oxidation of the prepared donor radicals gives rise to ground state triplet cation diradicals reflecting their unique electronic structure.[7] We also point out that the ground state spin multiplicity of heteroanalogues of π-conjugated spin systems is not necessarily predicted by Ovchinnikov's rule.[8] The spin correlation in singly oxidized donor radicals, however, is found to be rationalized by Borden's criterion on the basis of their space-sharing nature of two types of SOMOs (singly occupied molecular orbitals).[9] Finally, application of the novel spin system derived from spin-polarized donors is documented.

Results

1. Preparations of Donor Radicals. Amine-based donor radicals (**DMANN**, **DEANN**, and **MORNN**) were prepared by treating bromo nitronyl nitroxide **2** with the corresponding secondary amines (Scheme 2a). Aminophenyl-based donor radicals with a different substitution pattern (**p**&**mAPNN**) were synthesized from the corresponding formyl derivatives **3** and **7** (Scheme 2b). As for the *m*-formyl derivative **7**, the corresponding ester **5** was reduced to *m*-dimethylaminobenzyl alcohol **6**, which was oxidized by pyridinium chlorochromate to afford the desired compound (see Experimental Section). The ring-closure reaction of formyl compounds **3** and **7** with bishydroxylamine was catalyzed by bishydroxylamine sulfate to afford cyclic hydroxylamines **4** and **8**, respectively, in high yields. Cyclic hydroxylamines **4** and **8** were oxidized by PbO_2 to yield **p**- and **mAPNN**, respectively.

(7) (a) Kumai, R.; Matsushita, M. M.; Izuoka, A.; Sugawara, T. *J. Am. Chem. Soc*. **1994**, *116*, 4523−4524. (b) Kumai, R.; Sakurai, H.; Izuoka, A.; Sugawara, T. *Mol. Cryst. Liq. Cryst*. **1996**, *279*, 133−138. (c) Sakurai, H.; Kumai, R.; Izuoka, A.; Sugawara, T. *Chem. Lett*. **1996**, 879−880. (d) Sakurai, H.; Izuoka, A.; Sugawara, T. *Mol. Cryst. Liq. Cryst*. **1997**, *306*, 415−421. (e) Sugawara, T.; Izuoka, A. *Mol. Cryst. Liq. Cryst.* **1997**, *305*, 41−54.

(8) Ovchinnikov, A. A. *Theor. Chim. Acta (Berl.)*. **1978**, *47*, 297−304.

(9) (a) Borden, W. T. *Mol. Cryst. Liq. Cryst*. **1993**, *232*, 195−218. (b) *Magnetic Properties of Organic Materials*; Lahti, P. M., Ed.; Marcel Dekker: New York, 1999; pp 61−102.

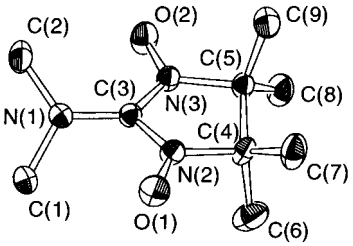

Figure 1. ORTEP drawing of the molecular structure of **DMANN** at 30% probability.

Table 1. Selected Bond Lengths, Bond Angles, and Torsion Angles for **DMANN** and **pAPNN** in **pAPNN·CA**

	DMANN	**pAPNN** in **pAPNN·CA**	
Bond Lengths (Å)			
O(1)−N(2)	1.282(3)	O(1)−N(2)	1.268(10)
O(2)−N(3)	1.289(3)	O(2)−N(3)	1.296(10)
C(3)−N(3)	1.342(3)	C(9)−N(3)	1.34(1)
C(3)−N(2)	1.341(4)	C(9)−N(2)	1.39(1)
Bond Angles (deg)			
C(1)−N(1)-C(3)	119.0(3)	C(1)−N(1)-C(3)	123.5(9)
C(1)−N(1)-C(2)	118.1(3)	C(1)−N(1)-C(2)	117.2(8)
C(2)−N(1)-C(3)	121.4(3)	C(2)−N(1)-C(3)	119.3(9)
Torsion Angles (deg)			
C(1)−N(1)-C(3)−N(2)	47.1(4)	C(2)−N(1)-C(3)−C(5)	0(1)
C(2)−N(1)-C(3)−N(3)	32.3(4)	C(1)−N(1)-C(3)−C(4)	−3(1)
		C(6)−C(8)-C(9)−N(2)	2(1)
		C(6)−C(8)-C(9)−N(3)	−1(1)
Dihedral Angle (deg)			
		between plane 1−2[a]	1.23

[a] Plane 1 is a least-squares plane consisting of C(3)−C(4)-C(5)−C(6)-C(7)−C(8), and plane 2 is of C(9)−N(2)-N(3)−O(1)-O(2).

2. Molecular Structures of Donor Radicals. The molecular structure of neutral **DMANN** was determined by X-ray crystallographic analysis. Crystallographic parameters are given in the Experimental Section. An ORTEP drawing of the **DMANN** molecule is shown in Figure 1 with the numbering scheme. The selected bond lengths, bond angles, and torsion angles with their estimated standard deviations are listed in Table 1. The bond lengths, O(1)−N(2) and O(2)−N(3), C(3)−N(3) and C(3)−N(2) are equal within the standard deviations. The twist angle (cf. θ in Figure 13) between the dimethylamino group with a shallow pyramidal form and the nitronyl nitroxide group is ca. 40°.

A charge transfer complex composed of **pAPNN** and chloranil (**CA**) was prepared by mixing benzene solutions of **pAPNN** and **CA** in a 1:1 molar ratio, followed by slow evaporation of the solvent at room temperature. Single crystals of the CT complex (**pAPNN·CA**) were obtained as small thin plates. This CT complex can be regarded as a model to discuss the molecular structure of **pAPNN** in the singly oxidized state. Crystallographic parameters of **pAPNN·CA** are summarized in the Experimental Section, although the quality of the collected crystallographic data is poor due to the kinetic instability of the complex. An ORTEP drawing of **pAPNN** in the CT complex is shown in Figure 2a with a numbering scheme. The selected bond lengths, bond angles, and torsion angles with their estimated standard deviations are listed in Table 1. The dihedral angle between the phenyl ring and the nitronyl nitroxide ring is 0.78°. While **pAPNN** exists as a twist form in the neutral crystal,[10] it turns out to be almost planar in **pAPNN·CA**. The crystal structure of **pAPNN·CA** is displayed in Figures 2b and 2c. Planar **pAPNN**s and acceptor molecules (**CA**s) are stacked alternately along the *c* axis (Figure 2b), and the distance between

(10) Caneschi, A.; Gatteschi, D.; le Lirzin, A. *J. Mater. Chem*. **1994**, *4*(2), 319−326.

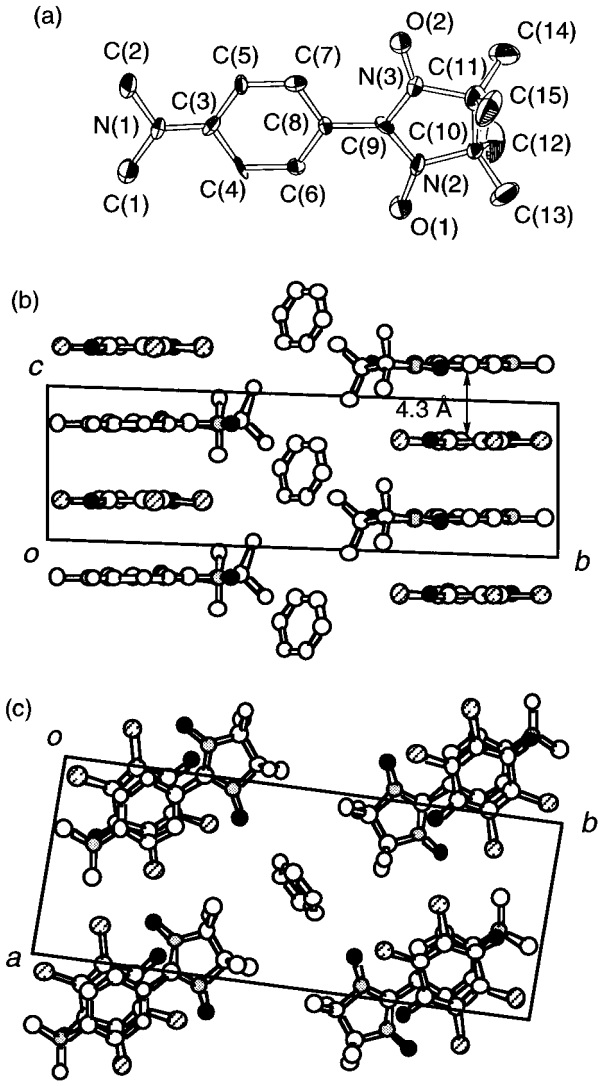

Figure 2. (a) ORTEP drawing of the molecular structure of **pAPNN** in **pAPNN·CA** at 30% probability and (b) crystal structure of **pAPNN·CA**: view along the *a* axis, (c) in the *ab* plane.

Table 2. Oxidation Potentials of Donor Radicals and Reference Compounds vs Ag/AgCl

compounds	$E_{1/2}{}^a$/V	compounds		$E_{1/2}{}^a$/V
NNH	0.82			
dimethylamine	1.27 (irr.)	**DMANN**	0.53	
diethylamine	1.49 (irr.)	**DEANN**	0.60	
morpholine	1.25 (irr.)	**MORNN**	0.58	
dimethylaniline	0.82 (irr.)	**pAPNN**	0.64	1.31 (irr.)
		mAPNN	0.75	1.17 (irr.)

[a] Experimental condition: acetonitrile solution in the presence of 0.1 M tetra-*n*-butylammonium perchlorate as a supporting electrolyte; scanning rate was 200 mV·s^{-1}.

the aromatic ring and the quinone ring is ca. 4.3 Å. Viewed along the *c*-axis, the benzene ring of **pAPNN** and the quinone ring of **CA** overlap each other almost completely (Figure 2c). A benzene molecule is incorporated within a cavity created by the methyl groups of the nitronyl nitroxide moieties of the facing **pAPNN**s (Figures 2b and 2c).

3. Electrochemical Properties of Donor Radicals. Oxidation potentials of the five donor radicals prepared here were determined by cyclic voltammetry. The half-wave potentials are listed in Table 2, together with those of the reference compounds. The first oxidation potentials of amine- or aminophenyl-based donor radicals are between 0.53 and 0.75 V, while those of the reference donor compounds are between 0.82 and 1.49 V and 0.82 V for 2-hydro-4,4,5,5-tetramethylimidazoline-3-oxide-1-oxyl (**NNH**). It is to be noted that the oxidation potentials of all the donor radicals composed of a donor unit and a radical unit are lower than those of the parent compounds. Among them, **DMANN** turned out to have the lowest oxidation potential of 0.53 V.

Table 3. *g* Values and hfc Constants of Donor Radicals in THF Measured at 30 K

	g_x	g_y	g_z	$a_z{}^N$ (2 N)/mT
DMANN	2.0105	2.0062	2.0016	1.88
DEANN	2.0105	2.0069	2.0012	1.87
MORNN	2.0102	2.0069	2.0011	1.84
pAPNN	2.0117	2.0055	2.0013	1.81
mAPNN	2.0114	2.0060	2.0012	1.86

4. Triplet ESR Spectra of Cation Diradicals Derived from Donor Radicals. The ESR spectra of neutral donor radicals in THF matrices were measured at 30 K. The spectrum of **DMANN** in a THF matrix showed the anisotropic *g* values $g_x = 2.0136$, $g_y = 2.0062$, and $g_z = 2.0016$ and the hyperfine structure of $a_z{}^N = 1.88$ mT (2 N) on the *z*-line.[11] The *g* values and the hyperfine coupling (hfc) constants of other donor radicals are listed in Table 3.

The cation diradical of **DMANN** was generated by addition of the excess iodine to a THF solution of **DMANN** at room temperature. The ESR spectrum of **DMANN**$^{+\bullet}$ in a frozen matrix is shown in Figure 3a. The resonance lines assignable to a triplet species were observed at 292.9, 305.8, 310.5, 335.0, 340.3, and 353.5 mT. The triplet signals were tentatively assigned to a pair of *X*, *Y*, and *Z* lines as shown in the figure. The zero-field splitting parameters calculated from these resonance fields were $|D| = 0.0276$ cm^{-1} and $|E| = 0.0016$ cm^{-1}. These parameters are summarized in Table 4 together with the g_{av} values which were calculated as $(g_x + g_y + g_z)/3$. Compared to other lines, the *Z*-line was rather broad presumably because of the presence of hfc of the nitrogen nuclei. Final chemical consequence of the singly oxidized **DMANN** was examined based on ESR spectroscopic data.[12] The temperature dependence of the low-field *Y*-line signal intensity followed the Curie law in the temperature range of 8−100 K (Figure 3b).

One-electron oxidation of the other donor radicals, **DEANN**, **MORNN**, **pAPNN** and **mAPNN**, afforded similar triplet ESR spectra as in the case of **DMANN**. The temperature dependence of the triplet ESR signal intensities of these donor radicals also obeyed Curie law. Figures 4a and 4b show the triplet ESR spectrum of an oxidized species of **mAPNN** and the Curie plot of the triplet signal, respectively. Calculated zero-field splitting parameters and anisotropic *g* values for all the observed triplet species are shown in Table 4. All the values were about the same as those of **DMANN**$^{+\bullet}$.

5. Physical Properties of a Charge Transfer Complex Composed of a Donor Radical. The UV−NIR spectrum of a CT complex, **pAPNN·CA**, in a KBr pellet showed a broad peak at around 11000 cm^{-1} (1.4 eV) which was assignable to a charge

(11) The anisotropic *g* values are tentatively assigned to g_x, g_y and g_z according to the decreasing order.

(12) After warming the sample to room temperature, neither neutral **DMANN** or the singly oxidized **DMANN** was detected by the ESR measurement. The strong signal at the central magnetic field in the frozen sample, therefore, was ascribed to the decomposed compounds derived from the oxidized species. The ESR spectrum of the decomposed sample measured at room temperature was assigned to a mixture of two doublet species. The species at $g = 2.0064$ with the hyperfine structure of $a = 0.73$ mT coupled with two equivalent $I = 1$ nucleus. The other at $g = 2.0066$ of $a = 0.16$ mT of $I = 1$ with $a = 0.49$ mT with six equivalent $I = {}^1/_2$ nuclei.

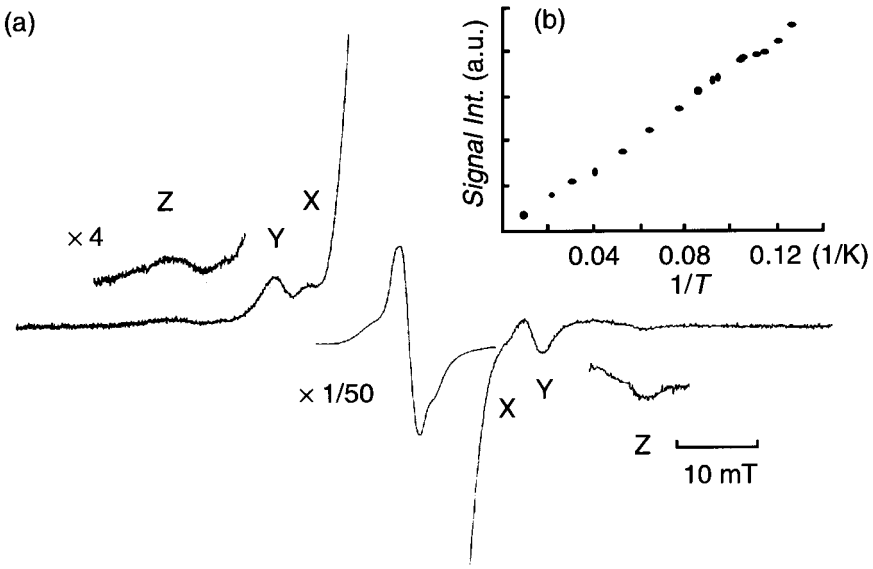

Figure 3. (a) ESR spectrum of **DMANN**$^{+\bullet}$ in THF matrix at 8 K. Central signals are due to the decomposed radicals.[12] (b) Temperature dependence of the signal intensity of **DMANN**$^{+\bullet}$.

Table 4. Zero-Field Splitting Parameters and g Values for Cation Diradicals in a THF Frozen Matrix at 8 K

	$\|D\|$/cm^{-1}	$\|E\|$/cm^{-1}	g_x	g_y	g_z	g_{av}
DMANN$^{+\bullet}$	0.0276	0.0016	2.0097	2.0077	2.0067	2.0080
DEANN$^{+\bullet}$	0.0273	0.0017	2.0069	2.0080	2.0073	2.0074
MORNN$^{+\bullet}$	0.0272	0.0018	2.0087	2.0067	2.0087	2.0080
pAPNN$^{+\bullet}$	0.0272	0.0018	2.0075	2.0066	2.0091	2.0077
mAPNN$^{+\bullet}$	0.0263	0.0020	2.0106	2.0088	2.0081	2.0092

transfer band. The IR spectrum of **pAPNN·CA** in the solid state showed the carbonyl stretching mode of **CA** at 1682 cm^{-1}. The position of the absorption band of the complex is close to those of the uni-component sample (1692 and 1681 cm^{-1}). The other peaks of the spectrum were also interpreted by the superposition of those of individual components of the complex.

The magnetic susceptibility of **pAPNN·CA** was measured by the Faraday method in a temperature range of 3−270 K. The magnetic property of the complex was basically paramagnetic with a weak antiferromagnetic interaction ($\theta = -0.8$ K). The Curie constant of 0.35 emu·K·mol^{-1} at higher temperatures was slightly less (7%) than 1 mol unit of $S = {}^1/_2$ spins. The electrical conductivity of **pAPNN·CA** was lower than 10^{-6} S·cm^{-1} at room temperature when measured by a two-probe method along the crystal c axis: The axis corresponds to the direction of the donor−acceptor stacking.

A charge-transfer complex (**DMANN·DDQ**) was obtained as a black powder by grinding **DMANN** ($E_{ox} = 0.53$ V) and 2,3-dichloro-5,6-dicyano-1,4-benzoquinone (**DDQ**) ($E_{red} = 0.59$ V).[13] All attempts to obtain single crystals have been unsuccessful. The VIS−NIR spectrum of the **DMANN·DDQ** complex in a KBr pellet showed a broad band from 10000 cm^{-1} to an IR region with a maximum absorption at 5300 cm^{-1} (0.65 eV), which was assignable to a CT band (Figure 5). The IR spectrum of **DMANN·DDQ** was totally different from those of the neutral compounds. The tail of the CT absorption band extended over to ca. 1700 cm^{-1} (0.21 eV), and most of the peaks in the range of 1700−500 cm^{-1} were broadened. The stretching of the cyano group of **DDQ** in the complex was observed at 2219 cm^{-1}, while those of neutral **DDQ** and **K**$^+$**DDQ**$^{-\bullet}$ were at 2234 and 2217 cm^{-1}, respectively.[14] The absorption position of the cyano stretching corresponds to that of the anion radical salt.[15]

(13) Toda, F.; Miyamoto, H. *Chem. Lett.* **1995**, 861.

Temperature dependence of the magnetic susceptibility of the complex was measured by the Faraday method in a temperature range of 3−270 K. The magnetic property of the complex was basically paramagnetic. The Curie constant was 0.31 emu·K·mol^{-1} at higher temperatures. This value was about 18% less than that of the $S = {}^1/_2$ radical. Although the $\chi_p \cdot T$ plot could not be reproduced by the Curie−Weiss equation throughout the temperature region measured, a weak antiferromagnetic interaction ($\theta = -1$ K) was at least detected from the plot at lower temperatures. The field dependence of the magnetization of the complex was measured at 3 K. The curve almost fitted the Brillouin function of $S = {}^1/_2$. Conductivity of the freshly prepared complex in a compressed pellet was measured by means of a two-probe method to showed a low conductivity of ca. 10^{-6} S·cm^{-1}) at room temperature.

Discussion

1. Molecular Structures of Donor Radicals in Uni-Component Crystals or in Charge Transfer Complexes. To discuss the molecular structure of a donor radical, an X-ray crystallographic analysis was performed on a single crystal of **DMANN**. From the fact that the bond lengths of O(1)−N(2) and O(2)−N(3), C(3)−N(3) and C(3)−N(2) are equal within the standard deviations, the nitrone and the nitroxide moieties are considered to be equivalent due to the resonance effect (Table 1). The twist angle between the direction of a lone pair of electrons of the dimethylamino group and the normal axis to the best plane of the nitronyl nitroxide group is ca. 40° (Figure 1). The twist may be caused not only by the steric repulsion between the methyl groups of the dimethylamino group and the oxygen atoms of the nitronyl nitroxide but also by the repulsive electronic interaction between a lone pair of electrons of the former group and a π-orbital of the latter. This means that if the twist angle becomes zero, the orbital energies, in particular that of HOMO of the eclipse conformer, must be raised because HOMO (highest occupied molecular orbital) has large coefficients at the heteroatoms involved in **DMANN** (see Appendix).

(14) Miller, J. S.; Krusic, P. J.; Dixon, D. A.; Reiff, W. M.; Zhang, J. H.; Anderson, E. C.; Epstein, A. J. *J. Am. Chem. Soc.* **1986**, *108*, 4459−4466.

(15) When the ratio of **DDQ** was increased, only signals of excess **DDQ** appeared in the spectrum of **DMANN·DDQ**, suggesting that **DMANN** and **DDQ** form a stable 1:1 complex.

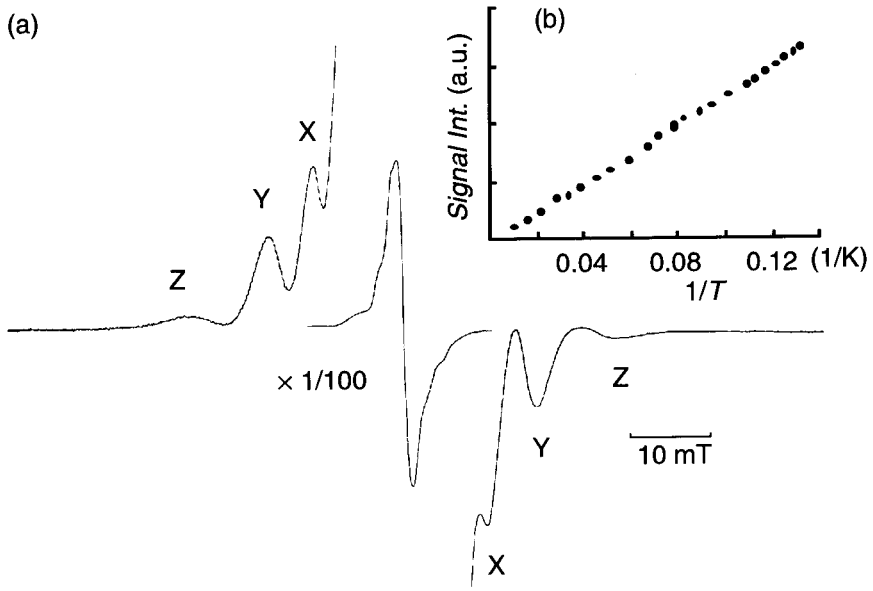

Figure 4. (a) ESR spectrum of **mAPNN**$^{+\bullet}$ in THF matrix at 8 K. Central signals are due to neutral **mAPNN**. (b) Temperature dependence of the signal intensity of **mAPNN**$^{+\bullet}$.

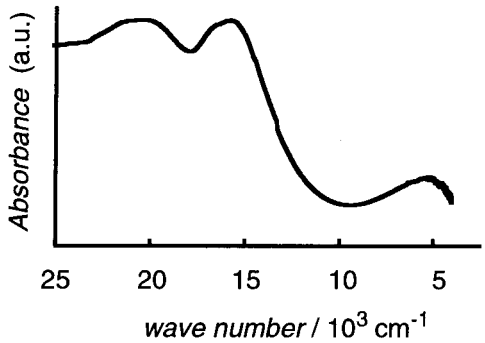

Figure 5. UV−NIR spectrum of **DMANN·DDQ** complex.

The crystal structure of neutral **pAPNN** has been reported by Gatteschi et al.[10] The unit cell of **pAPNN** contains two crystallographically independent molecules. The dihedral angles between the best plane of the O−N−C−N−O moiety and the phenyl ring of each **pAPNN** are 25° and 23° in a conrotatory manner. The result is consistent with the tendency that the dihedral angles of other *para*-substituted aromatic nitronyl nitroxides are usually larger than 20°; for example, 36° for *p*-fluorophenyl, 32° for *p*-iodophenyl, and 25° for *p*-chlorophenyl nitronyl nitroxide.[16] The reason for the twisting may be interpreted in the same manner as in the case of **DMANN**.

Contrary to the twisted molecular structure of the unicomponent **pAPNN**, the molecular structure of **pAPNN** in the charge transfer complex (**pAPNN·CA**) is almost planar (Figure 2b). The molecular packing shows that HOMO of the donor radical and LUMO (lowest unoccupied molecular orbital) of the acceptor molecule overlapped each other exactly in phase (Figure 2c) in a mixed-stack columnar structure (Figure 2b). This geometrical feature is consistent with the observation of a charge transfer band (11000 cm^{-1}) in the absorption spectrum of **pAPNN·CA**. Although several CT complexes composed of an organic radical and an acceptor are reported,[17] this may be the first example in which a π-donor radical and a π-acceptor are stacked alternately in a columnar structure. The complex is, however, considered to be almost neutral, judging from the difference between the redox potentials of the donor (E_{ox} = 0.64 V) and the acceptor (E_{red} = 0.09 V) and also from the IR spectral data as described in the Results section 5. The above results suggest that the molecular structure of the cation diradical derived from one-electron oxidation of a donor radical could also be planar.

2. PMO Analysis of Electronic Structure for Donor Radicals. The characteristic electronic structure of the cross-conjugated donor radical may be best understood by a perturbational molecular orbital (PMO) method.[18] Namely, a donor radical (e.g., **DMANN**) is composed by *union* of a donor molecule (e.g., dimethylamine) and a radical molecule (e.g., 2-hydro-4,4,5,5-tetramethylimidazoline-3-oxide-1-oxyl, **NNH**). The electronic structure of such a donor radical may be represented by either (a) or (b) as shown in Figure 6: The highest occupied molecular orbital of the donor, the singly occupied molecular orbital of the radical, and the next highest occupied molecular orbital of the radical are defined as *homo*, *somo*, and *homo*, respectively. In case (a), the *homo* of the donor and *somo* of the radical interact mutually, and the resulting singly occupied molecular orbital (SOMO) of the radical donor locates itself above the highest fully occupied molecular orbital (HOMO). On the other hand, in case (b), the *homo* of the donor and the *homo* of the radical interact mutually, not interacting with *somo* of the radical, because of the mismatch of the symmetry of the relevant partial molecular orbitals. Since this electronic interaction raises the energy level of the resultant HOMO of the donor radical, it may be possible to locate HOMO above SOMO. Such an exotic structure can be maintained, if the on-site Coulombic repulsion of SOMO is larger than the orbital energy difference (ΔE) between HOMO and SOMO. Whereas a donor radical of type (a) in Figure 6 should afford a closed shell cation species upon one-electron oxidation, one-

(16) (a) Hosokoshi, Y.; Tamura, M.; Kinoshita, M.; Sawa, H.; Kato, R.; Fujiwara, Y.; Ueda, Y. *J. Mater. Chem.* **1994**, *4*, 1219−1226. (b) Hosokoshi, Y. Ph.D. Thesis, The University of Tokyo, 1995.

(17) (a) Nakatsuji, S.; Takai, A.; Nishikawa, K.; Morimoto, Y.; Yasuoka, N.; Suzuki, K.; Enoki, T.; Anzai, H. *J. Mater. Chem.* **1999**, *9*, 1747−1754. (b)Sugimoto, T.; Tsujii, M.; Suga, T.; Hosoito, N.; Ishikawa, M.; Takeda, N.; Shiro, M. *Mol. Cryst. Liq. Cryst.* **1995**, *272*, 183−194. (c) Ishida, T.; Tomioka, K.; Nogami, T.; Iwamura, H.; Yamaguchi, K.; Mori, W.; Shirota, Y. *Mol. Cryst. Liq. Cryst.* **1993**, *232*, 99−102. (d) Sugano, T.; Fukasawa, T.; Kinoshita, M. *Synth. Met.* **1991**, *41*−*43*, 3281−3284.

(18) Borden, W. T.; Davidson, E. R. *J. Am. Chem. Soc.* **1977**, *99*, 4587−4594.

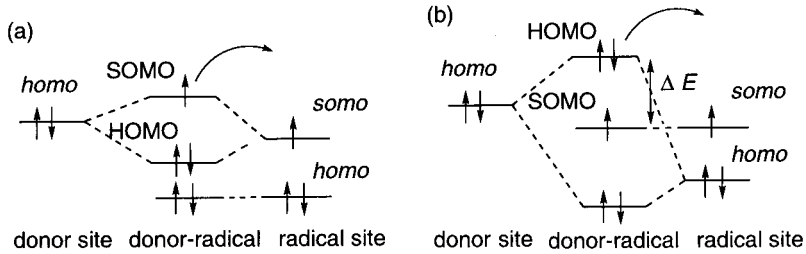

Figure 6. Schematic drawing of the electronic configuration of radicals carrying a donor unit. (a) *homo* of the donor site interacting with *somo* of the radical site. (b) *homo* of the donor site interacting with *homo* of the radical site.

electron oxidation of a donor radical of type (b) occurs from HOMO to afford an open-shell cation diradical (Figure 6b).

Next, we will discuss how **DMANN** satisfies the aforementioned requirements. As seen in the previous section, the oxidation potential of **DMANN** ($E_{ox} = 0.53$ V) is lower than those of dimethylamine ($E_{ox} = 1.27$ V) and **NNH** ($E_{ox} = 0.82$ V): The latter two are regarded as parent compounds of **DMANN**. The lowering of the oxidation potential reflects the electronic interaction between the two units. Moreover, the detection of a triplet signal in the ESR spectrum of the singly oxidized **DMANN** strongly suggests that the electronic structure of **DMANN** can be represented as case (b) in Figure 6. The proof for a large on-site Coulombic repulsion of SOMO of a nitronyl nitroxide derivative may be obtained from the fact that the nitronyl nitroxide group is reluctant to be reduced.[19] This may be because SOMO is localized only on the nitronyl nitroxide group.

The fact that triplet ESR spectra were observed in all the oxidized species in Table 4 indicates that their electronic structure can also be classified as the case shown by Figure 6b. It is to be stressed that close examination of the electronic feature of **DMANN** and other amine-based donor radicals gives a clue for the design of a donor radical which affords a ground state triplet species upon one-electron oxidation.

3. Origin of Ferromagnetic Coupling in Cation Diradicals Derived from Spin-Polarized Donors. The Curie plot of the triplet signal of **DMANN**$^{+\bullet}$ afforded a straight line in the temperature range of 8−100 K (Figure 3b). The experimental result strongly suggests that the oxidized species exists as a cation diradical with a triplet ground state. To rationalize the ground state of the cation diradical derived from a donor radical, a molecular orbital calculation was performed on the cation diradical of **DMANN** using a PM3/RHF method. Two singly occupied molecular orbitals of **DMANN**$^{+\bullet}$ correspond to nonbonding molecular orbitals (NBMOs) of alternate hydrocarbons (trimethylmethane, **TMM** for example), although the degeneracy was removed by lower symmetry.[20] Coefficients of the singly occupied molecular orbitals of **DMANN**$^{+\bullet}$ are displayed in Figure 7 together with those of NBMOs of **TMM**. As can be seen from Figure 7, coefficients of SOMO are restricted on the nitronyl nitroxide group, while those of SOMO′, which are derived from one-electron oxidation of HOMO, spread over the entire molecule. Since the coefficients of SOMO are shared by those of SOMO′ especially at the nitronyl nitroxide group, they can be designated as space-sharing type molecular orbitals. The cation diradicals which have such space-sharing SOMOs, therefore, should have a positive exchange interaction

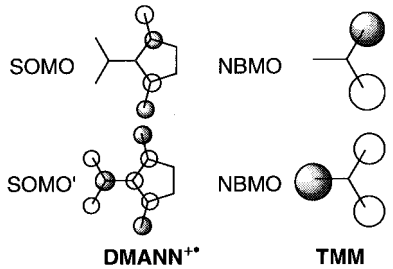

Figure 7. Coefficients of singly occupied molecular orbitals for **DMANN**$^{+\bullet}$ and **TMM** calculated by the PM3/RHF method.

between two unpaired electrons. As far as the distribution of the coefficients of the singly occupied molecular orbitals for **DMANN**$^{+\bullet}$ is concerned, SOMO and SOMO′ closely resemble two degenerated NBMOs of **TMM** (Figure 7). Exchange interactions in **DEANN**$^{+\bullet}$ and **MORNN**$^{+\bullet}$ can be discussed in the same manner.

The zero-field splitting parameters of **DMANN**$^{+\bullet}$ were $|D| = 0.0276$ cm^{-1} and $|E| = 0.0016$ cm^{-1} as summarized in Table 4. The calculated D value for the presumed average distance (2.1 Å) between two unpaired electrons is 0.28 cm^{-1}.[21] This value is substantially larger than the observed one (0.0276 cm^{-1}). The discrepancy can be rationalized by considering the negative spin density on the α-carbon of the nitronyl nitroxide group.[22] In fact, the experimentally determined D value of **TMM** in a hexafluorobenzene matrix[23] is also much smaller than the geometrically estimated one, and it is only 0.024 cm^{-1}, which is close to that of **DMANN**$^{+\bullet}$. Thus, the theoretical consideration described above and the results from the ESR measurement provide evidence for the close resemblance of the electronic structure between **DMANN**$^{+\bullet}$ and **TMM** of which the ground state triplet spin multiplicity was proved both theoretically[24] and experimentally.[4] Thus, the cation diradical of **DMANN** can be regarded as a heteroanalogue of **TMM**, although the degeneracy of SOMO and SOMO′ is removed in the former.[25]

It is worthwhile discussing the remarkable difference in

(19) The reduction potentials of **NNH** and phenyl nitronyl nitroxide are −0.78 and −0.82 V, respectively.

(20) A qualitative method for predicting the ground state of non-Kekulé hydrocarbons is documented by Borden.[9] According to this method, when the connectivity of two NBMOs are nondisjoint, i.e., whose NBMOs cannot be confined to separate atoms by any linear combination, the triplet state will be the ground state for this diradical.

(21) The distance between the "unpaired" electrons of **DMANN**$^{+\bullet}$ was defined as the distance between the center of two N−O groups and the aminium nitrogen atom and was evaluated from the molecular structure which was optimized by a molecular mechanics calculation.

(22) Zheludev, A.; Barone, V.; Bonnet, M.; Delley, B.; Grand, A.; Ressouche, E.; Rey, P.; Subra, R.; Schweizer, J. *J. Am. Chem. Soc*. **1994**, *116*, 2019−2027.

(23) Dowd, P. *J. Am. Chem. Soc*. **1966**, *88*, 2587−2589.

(24) Cramer, C. J.; Smith, B. A. *J. Phys. Chem*. **1996**, *100*, 9664−9670.

(25) The ground-state spin multiplicity of the hetero analogues of **TMM** has been calculated recently. (Li, J.; Worthington, S. E.; Cramer, C. J. *J. Chem. Soc., Perkin Trans. 2* **1998**, 1045−1051.) The ground state of iminoallyl which can be obtained by replacing the terminal carbon atoms of **TMM** with an imino group is calculated to be triplet. However, the energy difference between the triplet ground state and the singlet state becomes closer by 7 kcal/mol, compared to that of **TMM**. Moreover, the ground state of imium dimethylene diradical, which is isoelectronic with **DMANN**$^{+\bullet}$, was calculated to be singlet. Therefore, even if the ground state of **DMANN**$^{+\bullet}$ is triplet, the triplet−singlet energy difference is likely to be smaller than that of **TMM**.

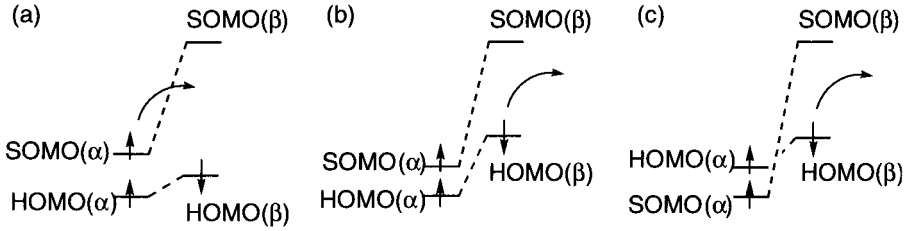

Figure 8. Electronic structures of (a) ordinary radical and (b, c) spin-polarized donor radical. The curved arrow represents an electron to be removed by one-electron oxidation.

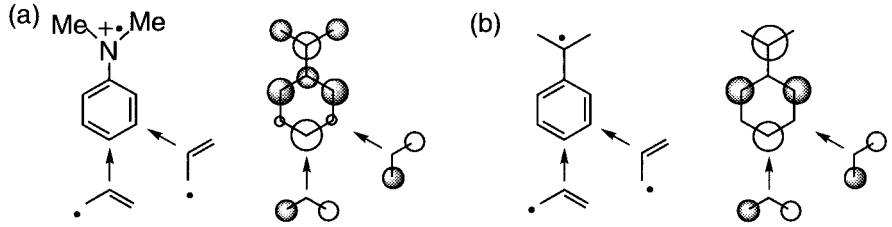

Figure 9. Distribution of coefficients of SOMOs of diradicals composed of (a) dimethylanilinium and allylic radicals and (b) benzyl radical allylic radicals.

kinetic stability between **DMANN**$^{+\bullet}$ and **TMM**. In the case of **TMM**, this diradical is photogenerated from a diazo precursor at liquid nitrogen temperature and it exists only at cryogenic temperatures. On the contrary, **DMANN**$^{+\bullet}$ can be generated at room temperature and it survives in a certain time period. Such a significant stabilization of the triplet diradical cation can be achieved by replacing the allyl radical unit with a nitronyl nitroxide group. However, our attempts to isolate cation radical salts derived from amine- or aminophenyl-based donor radicals have not been successful so far. To increase the intensity of triplet ESR signals, the oxidation conditions of spin-polarized donors by iodine have been thorously examined. The signal intensity turned out not to increase appreciably even when the oxidation was carried out at lower temperatures e.g. 0, −20, or −40 °C. On the contrary, the triplet signal was found to be increased by leaving the oxidized sample at room temperature for 30−60 s before freezing the sample. The result suggests that the concentration of the triplet cation diradical is not governed by the rate of its decomposition but by the rate of its generation from a CT complex between the donor-radical and iodine. When the temperature of the sample is lowered, the equilibrium between the ion radical salt and the charge transfer complex inclines to the complex side.

4. Spin Polarization in Donor Radicals Described by a UHF Method. The electronic structure of donor radicals was calculated by a UHF method in order to elucidate the characteristic of donor radicals more precisely. First, phenyl nitronyl nitroxide was selected as an ordinary radical for the comparison with amine-based donor radicals. The orbital energy of SOMO-(α) of phenyl nitronyl nitroxide is higher than those of HOMO-(α) and HOMO(*β*), although HOMO(*β*) is located slightly above HOMO(α) (Figure 8a). The energy difference between the HOMO(*β*) and HOMO(α) can be regarded as an energetic spin-polarization. Since the spin-polarization in phenyl nitronyl nitroxide is not large enough to locate HOMO(*β*) above SOMO-(α), one-electron oxidation of this radical will afford a closed-shell cationic species, removing an electron from SOMO(α). On the other hand, the energy level of HOMO(*β*) is located above SOMO(α), in the case of case (b) in Figure 8. As a result, one-electron oxidation will remove the electron of HOMO(*β*) to afford a ground state triplet species. The electronic structure of **DMANN** falls into this category especially in an eclipsed conformation. Here we define a donor radical in which HOMO-(*β*) is located above SOMO(α) as a spin-polarized donor. If the donor character is even more stronger, the orbital energies of both HOMO(α) and -(*β*) becomes higher than that of SOMO-(α) as represented in Figure 8c (see the next section for **pAPNN**).

5. Extension of Spin-Polarized Donors to an Aromatic System. To expand the *π*-electronic structure of a spin-polarized donor, aromatic amines are chosen as a donor unit. The electronic structure of a cation diradical of the aminophenyl-based donor radical, which was composed of *N*,*N*-dimethylanilinium and allyl radicals, was examined in terms of a PMO method.[18] Contrasting to the case of a benzyl radical, the electronic structure of which is characterized as an alternate hydrocarbon (Figure 9b), the coefficients of a dimethylanilinium radical distribute not only at the *ortho*- and *para*-positions but also at the *meta*, although the coefficient at the latter position is much smaller (Figure 9a). Consequently, the diradicals consisting of anilinium and allyl radicals can be classified as a nondisjoint type, regardless of the substitution positions. The ferromagnetic coupling between these two radical units, therefore, can be expected both in *para*- and *meta*-isomers.

The ground state of cation diradicals was examined more precisely in terms of a semiempirical molecular orbital calculation as in the case of amine-based donor radicals. According to the molecular orbital calculation using a PM3/UHF method, the energy level of HOMO(*β*) of **pAPNN** turns out to be the highest (Figure 8c).[26] Thus, the one-electron oxidation removes the *β*-spin of HOMO to afford a ground state triplet diradical. When coefficients of the SOMO and SOMO′ of **pAPNN**$^{+\bullet}$ are examined, it is found they share the atomic orbitals on the nitronyl nitroxide group (Figure 10a). According to Borden's criterion[9] such a species is thought to have a triplet ground state.

Spin correlation in the *meta*-substituted derivative is also discussed on the basis of Borden's criterion. Although the coefficients of SOMO and SOMO′ are shared by the atomic orbitals on the nitronyl nitroxide group in **mAPNN**$^{+\bullet}$ (Figure 10b), the overlap of the coefficients of SOMO and SOMO′ of **mAPNN**$^{+\bullet}$ is smaller than that in the *para*-substituted system. The ferromagnetic exchange interaction, therefore, is considered to be much smaller.

(26) See also: Yamaguchi, K.; Okamura, M.; Nakano, M. *Chem. Phys. Lett.* **1992**, *191*, 237−244.

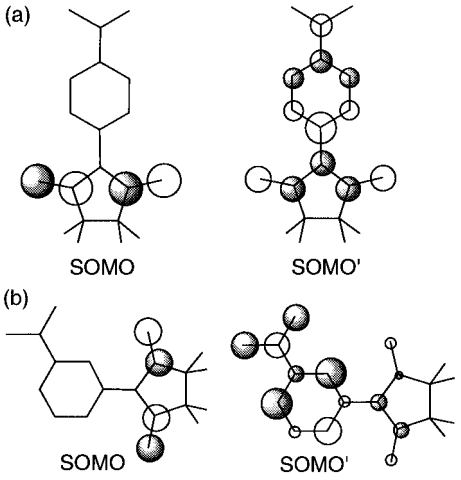

Figure 10. Coefficients of SOMO and SOMO′ of (a) **pAPNN**$^{+\bullet}$ and (b) **mAPNN**$^{+\bullet}$ calculated by a PM3/RHF method.

Oxidation of **pAPNN** and **mAPNN** by iodine afforded ESR spectra of the triplet species. Zero-field splitting (ZFS) parameters of these triplet species were not significantly different from those of the amine-based nitronyl nitroxides shown in Table 4. This may be because the ZFS parameter is governed by the spin distribution close to the nitronyl nitroxide group. The spin densities of **DMANN** and **pAPNN** calculated by a DFT method are depicted in Figure 11. The geminal dimethyl groups of NN were replaced by hydrogen atoms. As seen from the figure, the spin densities at the N−O groups, the C(2) carbon of the NN group, and the amino-nitrogen or the aromatic carbon atom at the foot of the NN group of **DMANN** or **pAPNN** are similar to each other. The tendency of the spin densities of these compounds can be understood by the canonical structures in the valence bond description (Scheme 3).

In the point-dipole approximation, the *D* value is estimated by the sum of the products of spin densities ($\rho_a \cdot \rho_b$) divided by $\langle r^3 \rangle$, where $\langle r \rangle$ is the average distance between the partial electron spins (spin densities). Therefore, the *D* values of **DMANN** and **pAPNN** are mainly governed by spin densities of the closer sites to the N−O groups aforementioned. Contribution from other sites should be much smaller because the average distances between the N−O groups and the other sites are substantially longer. Thus, it is not strange that the *D* values of **DMANN** and **pAPNN** are not significantly different from each other.

Since the temperature dependence of the triplet signal obeys the Curie law in the temperature range of 8−100 K, the ground state of **pAPNN**$^{+\bullet}$ is considered to be triplet, taking the result of molecular orbital calculation into account. On the other hand, the ground state of **mAPNN**$^{+\bullet}$ cannot be determined strictly. A triplet state may be the ground state or the energy difference between the triplet and the low-lying singlet is less than 10 cal/mol. The observation of the distinct triplet signal, however, is in contrast to a diradical of an odd alternate structure, because the substitution pattern of **mAPNN** is predicted to be singlet according to Ovchinikov's rule.[8] If the ground state of **mAPNN**$^{+\bullet}$ is triplet, introduction of heteroatoms may produce a novel spin system which cannot be achieved by hydrocarbon analogues.[27] The difference in the spin-polarization between **mAPNN**$^{+\bullet}$ and the corresponding hydrocarbon diradical (Figure 9b) may be derived from the significant contribution of coefficients at the *meta* positions of the aminium radical as stated above.

6. Charge Transfer Complexes Composed of Spin-Polarized Donors. It has been reported that some donor radicals form charge transfer complexes with acceptors.[17] The magnetic properties of those complexes were examined, and a part of them exhibited ferromagnetic intermolecular interaction. The electronic feature of those donor radicals, however, has not been fully elucidated, that is, whether an unpaired electron on the radical site has a ferromagnetic coupling with a π-electron spin generated by one-electron oxidation of the donor part. In this respect, it is interesting to study the magnetic properties of a CT complex of the spin-polarized donor, because it is proved to afford a ground state triplet species upon one-electron oxidation.

On the basis of the temperature dependence of the magnetic susceptibility, **pAPNN·CA** turned out to be a paramagnet. This may be because the ground state of the complex is basically neutral (see Results section 5). If the degree of the charge transfer is large enough to afford a ionic ground state, the complex is expected to provide a ferrimagnetic property (Figure 12a).[28] Although the CT complex with 2,3,5,6-tetrafluoro-7,7,8,8-tetracyanoquinodimethane (**TCNQ-F4**) was prepared,[17d] the paramagnetic spins were found to have almost disappeared, presumably due to the decomposition of the cation diradical.

To obtain a CT complex of an ionic type,[29] **DMANN** of lower oxidation potential (E_{ox} = 0.53 V) and **DDQ** (E_{red} = 0.59 V) were used (cf., the oxidation potential of **pAPNN** is 0.64 V and the reduction potential of **CA** is 0.11 V) The spectral data were consistent with the ionic character of the complex (see Results. 5). The temperature dependence of the magnetic susceptibility of the **DMANN·DDQ** complex revealed that the complex, however, is paramagnetic. The Curie constant of the complex was almost constant at 0.31 emu·K·mol^{-1} in the temperature range of 20−250 K. Incidentally, the $\chi_p \cdot T$ value at higher temperatures was ca. 18% less than one paramagnetic spin per complex. The lack of the expected value is caused by the decomposition of the complex, since the **DMANN·DDQ** complex turned out to be kinetically unstable. The result of the magnetic measurement may be interpreted as follows: In this complex, there are three kinds of spins; **D**$^{+\bullet}$, a cation radical on the donor site of **DMANN**; **R**$^{\bullet}$, a localized spin on the radical site of **DMANN**; **A**$^{-\bullet}$, and an anion radical of **DDQ**. Judging from the Curie constant, electron spins of the cation radical (**D**$^{+\bullet}$) and the anion radical (**A**$^{-\bullet}$) are supposed to be coupled strongly in an antiferromagnetic manner, leaving the spin (**R**$^{\bullet}$) on the radical site as a paramagnetic spin. Such an undesirable interaction may be derived from a tight overlap between the donor site of **DMANN** and **DDQ**, although no structural information is available at the present stage.

Yamaguchi has claimed that ferrimagnets may be constructed when a triplet cation diradical and a doublet anion radical are stacked alternately, with an antiferromagnetic interaction between them (Figure 12a).[28] If triplet cation radicals and anion radicals stack separately in a mixed valent state, even a conducting ferromagnet may be realized (Figure 12b). Although it is possible for the **DMANN·DDQ** complex to satisfy either of the requirements, the complex, in fact, exhibited neither ferro- nor ferrimagnetic intermolecular interactions. The discrepancy

(27) Okada, K.; Imakura, T.; Oda, M.; Kajiwara, A.; Kamachi, M.; Yamaguchi, M. *J. Am. Chem. Soc*. **1997**, *119*, 5740−5741.

(28) Yamaguchi, K.; Namimoto, H.; Fueno, T.; Nogami, T.; Shirota, Y. *Chem. Phys. Lett.* **1990**, *166*, 408−414.

(29) (a) Sugimoto, T.; Tsujii, M.; Murahashi, E.; Nakatsuji, H.; Yamaguchi, K.; Fujita, H.; Kai, Y.; Hosoito, N. *Mol. Cryst. Liq. Cryst.* **1993**, *232*, 117−134. (b) Nakamura, Y.; Koga, N.; Iwamura, H. *Chem. Lett*. **1991**, 69−71.

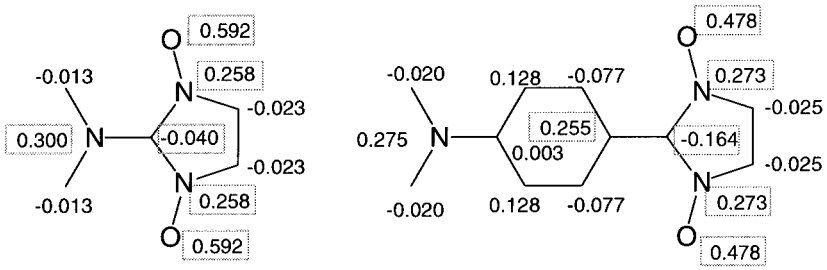

Figure 11. Spin densities of **DMANN**$^{+\bullet}$ calculated by a DFT method. Spin densities of **pAPNN**$^{+\bullet}$ are also depicted.

Scheme 3. Structures of **DMANN**$^{+\bullet}$ and **pAPNN**$^{+\bullet}$

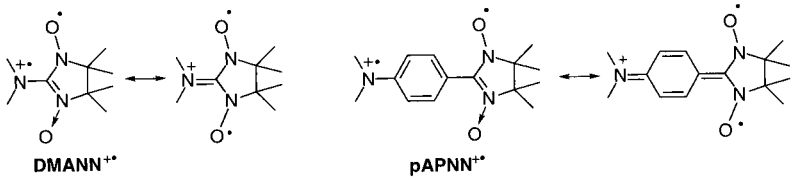

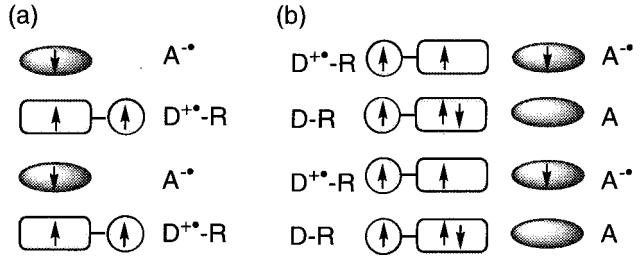

Figure 12. Schematic drawing of charge transfer complexes composed of spin-polarized donor. (a) Ferrimagnetic spin system and (b) conducting ferromagnetic spin system.

may be derived from the fine structure of the complex. If **DMANN**$^{+\bullet}$ and **DDQ**$^{-\bullet}$ are strongly dimerized, the antiferromagnetic interaction between the cation diradical and the anion radical may become even larger than the ferromagnetic intramolecular interaction between the π-spin on the donor site of **DMANN** and the localized spin on the radical site. In such a case, a ferrimagnetic spin ordering is not achieved. Consequently, the structural requirement should be examined more precisely in order to a realize ferrimagnetic spin system as shown in Figure 12a. Isolation of the ionic type complexes of the amine-based spin-polarized donors has so far not been successful. Recently, we have prepared TTF-based spin-polarized donors and have examined the conditions to isolate a charge transfer complex and/or ion-radical salts derived from the new type of donor radicals.[30]

At any rate, the CT complex composed of a spin-polarized donor and an acceptor has been prepared, and the ionic complex exhibits a conducting property. If the ion radical salt of a segregated columnar stacking type with mixed valency is formed using a spin-polarized donor and an acceptor with a reasonably high reduction potential, the salt may exhibit both metallic conductivity and ferromagnetism. It is to be stressed that the spin-polarized donors which we presented here are promising building blocks to construct a novel spin system.

Summary

To construct a novel high-spin system which can be generated by redox processes, amine-based donor radicals (e.g., **DMANN**) have been synthesized. Such a donor radical turned out to afford a ground state triplet cation diradical upon one-electron oxidation even at room temperature. Since two parallel spins in **DMANN**$^{+\bullet}$ reside on nondegenerated molecular orbitals, its electronic structure resembles that of a photoexcited triplet state of an organic π-molecule. In other words, the electronic structure of the photoexcited triplet state (T_0) was stabilized into a ground state according to a sophisticated molecular design. Such an exotic electronic structure can be maintained by virtue of a large Coulombic repulsion of SOMO and of a relatively small difference in the orbital energies of SOMO and SOMO′. Such type of donor radicals was designated as spin-polarized donors.

The concept of a spin-polarized donor was successfully extended to aminophenyl-based donor radicals. A high-spin cation diradical species was observed even from *meta*-substituted dimethylaminophenyl nitronyl nitroxide (**mAPNN**$^{+\bullet}$). The observed tendency apparently violates the prediction by Ovchinnikov's rule,[8] when the rule is formally applied to the heteroanalogue of an odd alternate hydrocarbon. The apparent violation, however, can be rationalized by applying Borden's concept on the space-sharing molecular orbitals to the heteroatom-containing extended π-system.

The outcome of these spin-polarized donors will provide a novel spin system which is characteristic of organic materials. The difference in the electronic structure between **TMM** and the cation diradicals reported here (e.g., **DMANN**$^{+\bullet}$) is that the unpaired electrons of the diradical reside in two singly occupied molecular orbitals (SOMO) of different character. Accordingly, each unpaired electron in the nondegenerated SOMO plays an individual role, constructing a unique spin system. For example, if spin-polarized donors are stacked and partially doped, the conduction electron, which itinerates along the columnar stack of the donor units, may align local spins on the radical units ferromagnetically on the basis of the strong ferromagnetic intramolecular coupling.[31] The ferromagnetic transition temperatures of organic ferromagnetic metals composed of spin-polarized donors are, therefore, expected to be raised substantially higher than those of organic ferromagnets discovered so far.[32] Moreover, even an organic spin device may be constructed

(30) (a) Nakazaki, J.; Matsushita, M. M.; Izuoka, A.; Sugawara, T. *Tetrahedron Lett.* **1999**, *40*, 5027−5030. (b) Nakazaki, J.; Ishikawa, Y.; Izuoka, A.; Sugawara, T.; Kawada, Y. *Chem. Phys. Lett.* **2000**, *319*, 385−390.

(31) (a) Dormann, E.; Nowak, M. J.; Williams, K. A.; Angus, R. O., Jr.; Wudl, F. *J. Am. Chem. Soc.* **1987**, *109*, 2594−2599. (b) Yamaguchi, K.; Okamura, M.; Fueno, T. *Synth. Met.* **1991**, *41*−*43*, 3631−3634.

(32) Nogami, T.; Ishida, T.; Tsuboi, H.; Yoshikawa, H.; Yamamoto, H.; Yasui, M.; Iwasaki, F.; Iwamura, H.; Takeda, N.; Ishikawa, M. *Chem. Lett.* **1995**, 635−636 and references therein.

using a spin-polarized polyradical donors the spin multiplicity of which can be converted reversibly through redox processes.[33]

Experimental Section

General Methods. Gel permeation chromatography (GPC) was performed by LC908 or LC908-C60 (Japan Analytical Industry Co., Ltd.) equipped with JAIGEL-1H and -2H columns. Chloroform was used as an eluent. ^{1}H NMR spectra were measured by an α-500 (JEOL) spectrometer in chloroform-d_1 or dimethylsulfoxide-d_6 solutions. Chemical shifts were reported in δ relative to TMS, 0.00 ppm or dimethylsulfoxide, 2.49 ppm as an internal standard. Infrared spectra were recorded on a Perkin-Elmer 1400 series infrared spectrometer using KBr pellets. Elemental analyses were performed by YANACO CHN corder MT-5 at the Center of Organic Elemental Analyses in the University of Tokyo. Mass spectra were measured by a GCMS-QP1000 (Shimadzu) quadrupole mass-spectrometer (EI) in a direct ionization mode (70 V). Melting points were obtained with a MEL-TEMP II (Laboratory Devices) heating block and were uncorrected. Reflection spectra were recorded by a V-570 UV/VIS/NIR spectrophotometer (JASCO) using KBr pellets. Observed reflection spectra were converted to absorption spectra using a Kubelka−Munk transform.

X-ray Crystal Structure Analyses. Blue rod crystals of **DMANN** were obtained by slow evaporation of the solvent from a *n*-hexane solution. A single crystal with dimensions of 0.60 × 0.20 × 0.16 mm^3 was used for the X-ray analysis. The intensity data collection was performed at an ambient temperature on a Rigaku AFC-5 four-circle diffractometer using graphite-monochromatized Mo Kα radiation. Three standard reflections were measured for every 100 reflections and showed no significant variations throughout the data collection; 2616 reflections ($4° \le 2\theta \le 55°$) measured, 1123 independent reflections ($I > 3\sigma(I)$) were used for analysis. Structure was solved by direct methods (SAPI-91)[34] and Fourier techniques (DIRDIF-94).[35] The non-hydrogen atoms were refined anisotropically. The hydrogen atom coordinates were refined but their isotropic *B*'s were held fixed. Final refinement was performed with anisotropic thermal factors for all non-hydrogen atoms; 181 parameters, $R = 0.053$, $R_w = 0.063$, $S = 1.67$; maximum and minimum heights in final difference Fourier map 0.16 and −0.19 e$^-$/Å^3. Crystal data: $C_9H_{18}N_3O_2$, FW = 200.26, monoclinic, space group $P2_1/n$, $a = 11.083(4)$ Å, $b = 11.497(4)$ Å, $c = 9.263(3)$ Å, $\beta = 106.03(3)°$, $V = 1134.5(7)$ Å^3, $Z = 4$, $D_c = 1.172$ g/cm^3.

Bluish plate crystals of **pAPNN·CA** were prepared as described at a later part of the Experimental Section. A single-crystal having approximate dimensions of 0.80 × 0.28 × 0.01 mm^3 was used for the X-ray analysis. All measurements were performed at an ambient temperature on a Rigaku AFC7R diffractometer with graphite-monochromatized Mo Kα radiation. Three standard reflections were measured for every 150 reflections. The intensities were decreased by ca. 5% during the measurement. Of the 5591 reflections ($6° \le 2\theta \le 55°$) collected, 1419 reflections ($I > 3\sigma(I)$) were used for analysis. The structure was solved by direct methods (SHELX-86)[36] and Fourier techniques (DIRDIF-94).[35] Final refinement was performed with anisotropic thermal factors for all non-hydrogen atoms; 316 parameters, $R = 0.071$, $R_w = 0.053$, $S = 3.26$; maximum and minimum heights in final difference Fourier map 0.31 and −0.30 e$^-$/Å^3. Crystal data: $C_{24}H_{25}N_3O_4Cl_4$, FW = 561.29, triclinic, space group $P\bar{1}$, $a = 8.690(5)$ Å, $b = 22.16(2)$ Å, $c = 6.725(6)$ Å, $\alpha = 92.07(8)°$, $\beta = 90.51(8)°$, $\gamma = 91.41(5)°$, $V = 1293(1)$ Å^3, $Z = 2$, $D_c = 1.441$ g/cm^3.

The molecular and crystal structures in this paper were drawn by Moldraw.[37]

Electrochemical Measurements. Cyclic voltammograms were recorded in dry acetonitrile in the presence of 0.1 M tetra-*n*-butylammonium perchlorate (Nacalai Tesque, Inc.) as an electrolyte with a platinum working electrode using a potentiostat/galvanostat HAB 151 (Hokuto Denko Ltd.) at room temperature. An Ag/AgCl electrode was used for a reference electrode. Scanning rate was 200 mV·s^{-1}.

ESR Measurements. ESR spectra were measured on a JEOL JES-RE2X spectrometer (X-band microwave unit, 100 kHz field modulation) equipped with a liquid helium transfer system (Air Products and Chemicals, Inc., LTR-3). Temperature was controlled by a digital temperature indicator/controller (Scientific Instruments Inc., 3700). Temperature close to the sample was measured separately with a digital multithermometer (Advantest, TR2114H) with a gold−iron thermocouple (of an estimated precision of 0.5 K). Temperature calibration was performed by monitoring Ge resistance thermometer (Lake Shore, GR-200B-1500, in the temperature range of 6 to 100 K). Iodine was sublimed under a reduced pressure (ca. 5 mmHg). In a side arm portion made of Pyrex, was placed a THF solution (ca. 0.5 cm^3) of a large excess of iodine, and the solution was degassed by three freeze−thaw cycles through a high-vacuum stopcock (Flon Ind., F-6001 92-03). The solution was transferred to crystals of a donor radical (ca. 1 mg) which was placed at the bottom of a main-arm portion made of quartz. After shaking the mixed sample vigorously at room temperature, the sample tube was rapidly cooled in a precooled ESR cavity. The microwave frequency was measured with a TR5212 meter (Advantest), and the resonance magnetic fields of the signals were measured with the aid of an ES-FC5 NMR field meter (Echo Electronics). Dependence of the signal intensities on temperatures was measured by the use of a temperature-controlling accessory. Microwave power dependence of the signal intensities was checked by several power settings to avoid a power saturation at the low-temperature region.

Measurements of Magnetic Susceptibility. Magnetic susceptibilities of charge transfer complexes (**pAPNN·CA** and **DMANN·DDQ**) were measured by Faraday-type magnetic balance system (Oxford, 5 T).[38] The force loaded on the sample was measured by a Cahn 1000 electric microbalance. The quartz-basket containing the sample (ca. 10−15 mg) was hung from an electrobalance with a tungsten wire (0.08 mm ϕ) in a sample chamber of the cryostat. The outputs from the electricbalance system were processed by an NEC PC9801vm microcomputer, which was also used to control the temperature of the cryostat and the power supplied for the superconducting magnets.

Electrical Conductivity Measurement. A compaction pellet with a diameter of 3 mm of **DMANN·DDQ** was prepared by a compressor. The conductivity of **DMANN·DDQ** was measured by a two-probe method. For measuring the electric conductivity of the single crystal of **pAPNN·CA**, a two-probe method was used. Gold wires (25 μm ϕ) were attached to the sample with gold paste (Tokuriki Kagaku) as a contact.

Molecular Orbital Calculations. For semiempirical molecular orbital calculations, CAChe (including Editor, molecular mechanics, MOPAC, Tabulator, and Visualizer$^+$), a software provided by CAChe Scientific, Inc., was used. The geometrical structure was first optimized by molecular mechanics, and molecular orbital calculations using PM3 were conducted on a Power Macintosh 8500/120 computer.

Materials. Most of the chemicals were purchased from Tokyo Kasei Kogyo Co. Ltd., Wako Pure Chemicals Industries Ltd., and Aldrich Chemical Co. Inc. (Japan). Preparation of 2,3-bis(hydroxylamino)-2,3-dimethylbutane and 2,3-bis(hydroxylamino)-2,3-dimethylbutane sulfate were performed according to the published procedures.[39] Diethyl ether was distilled under nitrogen from sodium benzophenone ketyl before use. Dichloromethane was dried over molecular sieves (3 Å). Deactivated silica gel (Fuji Silysia Chemical Co., Ltd., BW-820MH) was prepared by the treatment with methanol before use. Florisil (100−200 mesh) was purchased from Katayama Chem. Co. Ltd., and Celite (No. 545) was purchased from Wako Pure Chemicals Industries Ltd.

(33) (a) Nakamura, T.; Momose, T.; Shida, T.; Sato, K.; Nakazawa, S.; Kinoshita, T.; Takui, T.; Itoh, K.; Okuno, T.; Izuoka, A.; Sugawara, T. *J. Am. Chem. Soc*. **1996**, *118*, 8684−8687. (b) Rajca, S.; Rajca, A. *J. Am. Chem. Soc*. **1995**, *117*, 9172−9179.

(34) Fan, H.-F. *Structure Analysis Programs with Intelligent Control*; Rigaku Corporation: Tokyo, Japan, 1991.

(35) Beurskens, P. T.; Admiraal, G.; Beurskens, G.; Bosman, W. P.; de Gelder, R.; Israel, R.; Smits, J. M. M. *The DIRDIF-94 program system*; Technical Report of the Cryatallography Laboratory: University of Nijmegen, The Netherlands, 1994.

(36) Sheldrick, G. M. *Crystallographic Computing 3*; Sheldrick, G. M., Kruger, C., Goddard, R.. Eds.; Oxford University Press: 1985; pp 175−189.

(37) Molecular graphics for Machintosh: Cense, J.-M. *Tetrahedron Comput. Methodol*. **1989**, *2*, 65−71.

(38) Awaga, K.; Maruyama, Y. *Chem. Mat*. **1990**, *2*, 535−539.

(39) Lamchen, M.; Mittag, T. W. *J. Chem. Soc. C* **1966**, 2300−2303.

Dry benzene, which was distilled over sodium metal, was used especially for the preparation of charge-transfer complexes of donor radicals. Chloranil (**CA**) and 2,3-dichloro-5,6-dicyano-1,4-benzoquinone (**DDQ**) were recrystallized from dichloromethane and chloroform solution, respectively. All the other reagents were used as purchased without further purification.

Preparation. Amine- or aminophenyl-based donor radicals were synthesized from the corresponding compounds as shown in Scheme 1.

2-Bromo-4,4,5,5-tetramethylimidazoline-3-oxide-1-oxyl (2). In reference 40 **BrNN** was prepared from **NNH** by treating with Br_2 in carbon tetrachloride/pyridine or by treating bicarbonate solution of **NNH** with cyanogen bromide. The method described below was found to yield **BrNN** more conveniently even in a better yield.

To an ice-cooled solution of 2.10 g (52.5 mmol) of NaOH in 12 mL of water was added 2.8 g (17.5 mmol) of Br_2 dropwise. A mixture of 0.21 mg (1.3 mmol) of 2-hydro-4,4,5,5-tetramethylimidazoline-3-oxide-1-oxyl (**1**), 50 mL of ice−water, and 1.0 mL of NaOBr aq obtained by the above procedure were shaken for 30 s in a 500 mL separating funnel. The solution was extracted with 40 mL of dichloromethane twice, washed with 50 mL of water twice, dried over $MgSO_4$, and filtered off, and then the solvent was concentrated down to ca. 3 mL by a rotary evaporator. Concentration of the solution by a slow evaporation of the solvent at 0 °C under N_2 yielded 0.26 g of red-purple crystals of the desired product (yield 84%). The product was purified by GPC: ESR in benzene solution $a_N = 0.782$ mT (2 N) at $g = 2.0060$; IR (KBr pellet, cm^{-1}) 2991, 1448, 1413, 1374, 1360, 1171, 1132; mp 134−138 °C (decomp).

2-Dimethylamino-4,4,5,5-tetramethylimidazoline-3-oxide-1-oxyl (DMANN).[41] To an ice-cooled solution of 0.30 g (1.3 mmol) of **2** dissolved in 10 mL of water was added 4 mL of a 50% aqueous solution of dimethylamine. After stirring for 4 h at room temperature, the solution was extracted with two 30 mL portions of dichloromethane, washed with 30 mL of water, and dried over $MgSO_4$. After filtered off the desiccant, the solvent was evaporated under a reduced pressure. The obtained product was recrystallized from hot *n*-hexane to give 0.14 g of blue needles (yield 55%): ESR in benzene solution $a_N = 0.741$ mT (2 N) at $g = 2.0059$; IR (KBr pellet, cm^{-1}) 2986, 2932, 1595, 1329, 1207, 1127, 1062, 874, 539; mp 112−113 °C. Anal. (percent) calcd for $C_9H_{18}N_3O_2$, C 53.98, H 9.06, N 20.98, found C 53.70, H 8.80, N 20.80.

2-Diethylamino-4,4,5,5-tetramethylimidazoline-3-oxide-1-oxyl (DEANN). To an ice-cooled solution of 0.26 g (1.1 mmol) of **2** dissolved in 8 mL of water was added 3 mL of diethylamine. After stirring for 24 h at room temperature, the solution was extracted with 50 mL of dichloromethane, washed with water, dried over $MgSO_4$, and filtered off, and then the solvent was evaporated under a reduced pressure. The obtained product was dissolved in hot *n*-hexane and insoluble byproducts were separated. After a removal of the solvent, the residue was purified on deactivated silica gel using 3% methanol−diethyl ether as an eluent. Evaporation of the solvent gave 25 mg of blue needles (yield 10%): ESR in benzene solution $a_N = 0.747$ mT (2 N) at $g = 2.0060$; IR (KBr pellet, cm^{-1}) 2980, 2932, 1598, 1451, 1387, 1369, 1330, 1296, 1208, 1145, 1127, 1102, 1088, 871, 541; mp 88.5−91.0 °C; EI-MS *m*/*e* 228 (M^+).

2-Morpholino-4,4,5,5-tetramethylimidazoline-3-oxide-1-oxyl (MORNN). To 10 mL of morpholine in a 30 mL round-bottomed flask cooled by an ice bath was added 210 mg (0.890 mmol) of **2**. After stirring the mixture for an hour, the ice bath was removed and the solution was stirred for overnight. Excess morpholine was removed under a reduced pressure at room temperature. The obtained product was dissolved in diethyl ether, and insoluble byproducts were separated. After a removal of the solvent, the residue was column chromatographed on silica gel using ethyl acetate as an eluent. The obtained product was recrystallized from *n*-hexane to give 100 mg of blue needles (yield 46%): ESR in benzene solution $a_N = 0.734$ mT (2 N) at $g = 2.0056$; IR (KBr pellet, cm^{-1}) 2985, 2900, 2856, 1595, 1368, 1340s, 1319s, 1260s, 1217, 1200, 1135, 1114s, 1004, 873, 857, 538; mp 151−152 °C; EI-MS *m*/*e* 242 (M^+). Anal. (percent) calcd for $C_{11}H_{20}N_3O_3$, C 54.53, H 8.32, N 17.35, found C 54.36, H 8.25, N 17.35.

2-(4′-Dimethylaminophenyl)-1,3-dihydroxy-4,4,5,5-tetramethylimidazolidine (4). Preparation of the cyclic hydroxylamine **4** was reported in reference 42. The addition of the hydroxylamine sulfate was found to afford the cyclic hydroxylamine **4** in higher yield by the procedure described below.

In a 50 mL round-bottomed flask, 600 mg (4.02 mmol) of 4-(dimethylamino)benzaldehyde **3**, 900 mg (6.08 mmol) of 2,3-bis-(hydroxylamino)-2,3-dimethylbutane, and 300 mg of 2,3-bis(hydroxylamino)-2,3-dimethylbutane sulfate as a catalyst were suspended in 30 mL of methanol. Between the neck of a reaction flask and a reflux condenser, a dropping funnel filled with molecular sieves (4 Å) was placed for dehydration. The reaction mixture was refluxed under nitrogen for overnight. After the solvent was concentrated to about half of the starting amount with a rotary evaporator, precipitates were filtered by suction and was washed with cold methanol. The obtained product was dried under a reduced pressure to give 1.12 g (94%) of colorless powders: ^{1}H NMR (DMSO-d_6, ppm) 7.58 (s, 2H), 7.41 (d, $J = 9$ Hz, 2H), 6.67 (d, $J = 9$ Hz, 2H), 4.39 (s, 1H), 2.85 (s, 6H), 1.04 (s, 6H), 1.02 (s, 6H); IR (KBr pellet, cm^{-1}) 3241 *br*, 2974, 2894, 1614, 1522, 1480, 1445, 1378, 1314, 1192, 1163, 1140, 804.

2-(4′-Dimethylaminophenyl)-4,4,5,5-tetramethylimidazoline-3-oxide-1-oxyl (pAPNN).[42] To a mixture of 500 mg (1.79 mmol) of cyclic hydroxylamine **4** and 30 mL of benzene were aded 500 mg of powdered anhydrous potassium carbonate and 2.0 g of PbO_2, and the suspension was stirred vigorously for 1.5 h. After filtering the reaction mixture through Celite, the solvent was removed by a rotary evaporator. The blue residue was chromatographed on a deactivated silica gel using chloroform as an eluent. The obtained product was recrystallized from hot ethanol to give 350 mg (yield 71%) of blue plates: ESR in benzene solution $a_N = 0.760$ mT (2 N) at $g = 2.0059$; IR (KBr pellet, cm^{-1}) 2985, 1608, 1498, 1387, 1369, 1358, 1298, 1207, 1132, 946, 815, 541; mp 153−154 °C. Anal. (percent) calcd for $C_{15}H_{22}N_3O_2$, C 65.19, H 8.02, N 15.21, found C 64.90, H 8.10, N 15.38.

3-(Dimethylamino)benzyl Alcohol (6).[43] In a 100 mL three-necked round-bottomed flask fitted with a 50 mL dropping funnel with a pressure-equalization arm and a reflux condenser equipped with a nitrogen balloon were placed with 1.30 g (34.0 mmol) of lithium aluminum hydride and 80 mL of anhydrous diethyl ether. After refluxing the suspended mixture for an hour, the dropping funnel was charged with 10.0 g (55.8 mmol) of 3-(dimethylamino)benzoic acid methyl ester **5** dissolved in 30 mL of anhydrous diethyl ether. While the suspension was gently stirred under nitrogen, the solution of ester **5** was added dropwise at a rate maintaining a gentle reflux. When the addition was complete, the reaction mixture was refluxed for 3 h. Then 20 mL of ethyl acetate was added and the solution was refluxed for other 2 h. The gray reaction mixture was hydrolyzed by an addition of 1 mL of 1 N HCl and 1 mL of water. The reaction mixture was filtered through Celite, washed with diethyl ether, dried over $MgSO_4$, and filtered off, and the solvent was evaporated under a reduced pressure. The obtained yellow oil (4:3 mixture of benzyl alcohol and a chlorinated compound) was dissolved in 40 mL of ethanol and was added to NaOH aq (80 g, 0.20 mol in 40 mL of water). After refluxing the mixture for 1.5 h, 100 mL of water was added. The obtained product was extracted by 400 mL of diethyl ether, washed with water, and dried over $MgSO_4$. After the evaporation of the solvent, 6.87 g (yield 81%) of yellow oil was obtained. No further purification was performed before the next step: ^{1}H NMR ($CDCl_3$, ppm) 7.23 (t, $J = 8$ Hz, 1H), 6.75 (d, $J = 2$ Hz, 1H), 6.71 (d, $J = 7$ Hz, 1H), 6.68 (dd, $J = 8$ and 2 Hz, 1H), 4.65 (s, 2H), 2.96 (s, 6H); IR (KBr pellet, cm^{-1}) 3364 br, 2873, 2803, 1606, 1582, 1499, 1439, 1352, 997, 776, 694.

3-(Dimethylamino)benzaldehyde (7). In a 200 mL round-bottomed flask, 1.34 g (8.86 mmol) of benzyl alcohol **6** was dissolved in 50 mL

(40) Boocock, D. G. B.; Ullman, E. *J. Am. Chem. Soc*. **1968**, *90*, 6873−6874.

(41) Ullman, E. F.; Call, L.; Leute, R. K.; Osiecki, J. H. U.S. Patent 3,740,412 (Cl.260−309.6; C07d), 1973.

(42) Ullman, E. F.; Osiecki, J. H.; Boocock, D. G. B.; Darcy, R. *J. Am. Chem. Soc*. **1972**, *94*, 7049−7059.

(43) Tsuchiya, M.; Yoshida, H.; Ogata, T.; Inokawa, S. *Bull. Chem. Soc. Jpn.* **1969**, *42*, 1756−1757.

(44) Cocker, W.; Harris, J. O.; Loach, J. V. *J. Chem. Soc*. **1938**, 751−753.

of dry dichloromethane. To this flask were added 2 mL of dry pyridine and 3.83 g (17.7 mmol) of powdered pyridinium chlorochromate. After an addition of 1.0 g (11 mmol) of powdered anhydrous sodium carbonate to the reaction mixture, the suspension was refluxed for overnight under nitrogen. When the mixture was cooled to room temperature, dry diethyl ether was added and the precipitates were filtered off through Florisil. The crude product was purified by GPC and then by silica gel column chromatography with $CHCl_3$ as eluent, giving 67 mg (yield 5%) of a yellow oil: ^{1}H NMR ($CDCl_3$, ppm) 9.96 (s, 1H), 7.39 (t, $J = 8$ Hz, 1H), 7.20 (d, $J = 8$ Hz, 1H), 7.19 (s, 1H), 6.97−6.99 (m, 1H), 3.02 (s, 6H); IR (KBr pellet, cm^{-1}) 2809, 1698s, 1602s, 1576, 1498, 1357, 1206, 998, 779, 683.

2-(3′-Dimethylaminophenyl)-1,3-dihydroxy-4,4,5,5-tetramethylimidazolidine (8). In a 50 mL round-bottomed flask, 217 mg (1.45 mmol) of **7**, 434 mg (2.93 mmol) of 2,3-bis(hydroxylamino)-2,3-dimethylbutane, and 100 mg of 2,3-bis(hydroxylamino)-2,3-dimethylbutane sulfate as a catalyst were dissolved in 20 mL of methanol. Between the neck of a reaction flask and a reflux condenser, a dropping funnel filled with molecular sieves (4 Å) was placed for dehydration. The reaction mixture was refluxed under nitrogen overnight. After the solvent was concentrated to about half of the starting amount with a rotary evaporator, precipitates were filtered by suction and was washed with cold methanol. The obtained product was dried under a reduced pressure to give 345 mg (yield 85%) of colorless powders: ^{1}H NMR ($CDCl_3$, ppm) 7.24 (d, $J = 8$ Hz, 1H), 6.91 (s, 1H), 6.90 (d, $J = 9$ Hz, 1H), 6.70−6.72 (m, 1H), 4.92 (s, 2H), 4.73 (s, 1H), 2.95 (s, 6H), 1.13 (s, 12H); IR (KBr pellet, cm^{-1}) 3265 br, 2981, 2912, 1608, 1504, 1378, 1218, 1145, 917, 776, 697.

2-(3′-Dimethylaminophenyl)-4,4,5,5-tetramethylimidazoline-3-oxide-1-oxyl (mAPNN). To a mixture of 193 mg (0.691 mmol) of cyclic hydroxylamine **8** and 10 mL of benzene were added 170 mg of powdered anhydrous potassium carbonate and 660 mg of PbO_2, and the mixture was stirred vigorously. The resulting colored mixture was stirred for 1 h. After filtering through Celite, the solvent was removed under a reduced pressure. The residue was column chromatographed on deactivated silica gel with 3% ethyl acetate−chloroform as an eluent. The obtained product was recrystallized from hot *n*-hexane to give 145 mg (yield 76%) of blue block crystals: ESR in benzene solution $a_N = 0.748$ mT (2 N) at $g = 2.0061$; IR (KBr pellet, cm^{-1}) 2982, 1580, 1575, 1493, 1454, 1415, 1395, 1360, 1216, 1190, 1165, 1137, 999, 856, 785, 688, 542; mp 105.0−105.5 °C; EI-MS *m*/*e* 276 (M^+). Anal. (percent) calcd for $C_{15}H_{22}N_3O_2$, C 65.19, H 8.02, N 15.21, found C 65.28, H 8.07, N 15.04.

Preparation of CT Complexes. pAPNN·CA:**pAPNN** (19 mg, 0.067 mmol) and chloranil (**CA**) (17 mg, 0.067 mmol) were dissolved separately in 0.6 and 1.4 mL of dry benzene, respectively. Each solution was filtrated and transferred into a 10 mL Erlenmeyer flask. The flask was kept standing in a desiccator in a dark cool place for 4 days. Small thin blue plates of **pAPNN·CA** were obtained after a slow evaporation of the solvent: IR (KBr pellet, cm^{-1}) 1682, 1603, 1563, 1540, 1416, 1366, 1299, 1215, 1132, 1112, 945, 835, 809, 741, 707. **DMANN·DDQ:** Grinding **DDQ** (2.0 mg, 0.0089 mmol) with crystals of **DMANN** (1.8 mg, 0.0089 mmol) by an agate mortar and pestle in an equal molar amount under a nitrogen atmosphere gave a black powder of **DMANN·DDQ**: IR (KBr pellet, cm^{-1}) 2219, 1675 br, 1500 br, 1412, 1225 br, 1188 br, 1038, 782, 509.

Acknowledgment. The authors gratefully acknowledge Dr. Reiji Kumai (Joint Research Center for Atom Technology) for helpful discussion and for the X-ray measurement of the **pAPNN·CA** complex. The authors are indebted to Prof. Kunio Awaga (The University of Tokyo) for his generous provision of the Faraday-type magnetic balance. This work was supported by CREST (the Core Research for Evolutional Science and Technology) of JST (the Japan Science and Technology Corp.) and by a Grant-in-Aid for Scientific Research on Priority Area "Molecular Magnetism" (Area No. 228/04 242 104) from the Ministry of Education, Science and Culture, Japan.

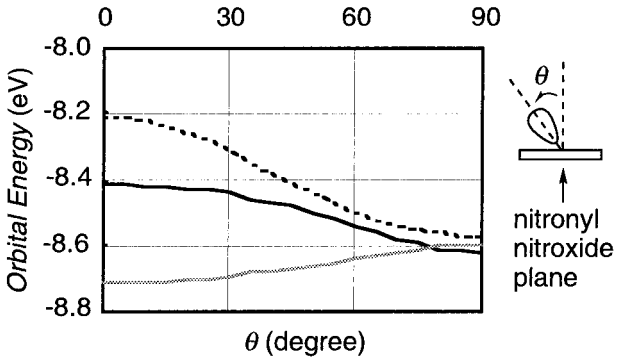

Figure 13. Angular dependence of the orbital energy for **DMANN**. (Dotted line, HOMO(β); solid line, HOMO(α); gray line, SOMO(α)).

Appendix

The heat of formation of **DMANN** was calculated using a PM3/UHF method, changing the angle (θ in Figure 13) between the direction of the lone pair of the amino group and the π-orbital of the nitronyl nitroxide group by every 5° in the range of 0−90°. The hybridization of the nitrogen atom of the amino group is fixed to sp^2 during the process. The most stable conformation was obtained with the twist angle of $\theta = 45°$, while the perpendicular conformation ($\theta = 90°$) turned out to be the least stable. This twist angle ($\theta = 45°$) was close to the value ($\theta \approx 40°$) that was obtained from the X-ray analysis. Preference of the twist conformation may be rationalized by the steric and electronic repulsion. Figure 13 shows the angular dependence of the orbital energy of HOMO(α) and HOMO(β) and SOMO(α). Judging from the calculated result, one-electron oxidation will remove a β-spin of HOMO to afford an open-shell cation diradical. Since the electronic interaction is largest at $\theta = 0°$, the largest spin-polarization of HOMO is obtained at this angle. Because the electrochemical oxidation of a donor radical in solution is considered to occur from a conformation with the lowest oxidation potential, the one-electron oxidation will occur when θ becomes close to 0°. In this conformation, oxidation must occur from HOMO(β) to afford the ground state triplet cation diradical as in Figure 8b.

Supporting Information Available: Crystal structure information for **DMANN** and **pAPPN·CA** (PDF). This material is available free of charge via the Internet at http://pubs.acs.org.

JA994547T